Review

Direct Use of Copper Slag as Photocatalytic Material for Solar Hydrogen Production

Susana Leiva-Guajardo *, Norman Toro, Edward Fuentealba, Mauricio J. Morel, Álvaro Soliz, Carlos Portillo, Felipe M. Galleguillos Madrid *

Posted Date: 10 July 2024

doi: 10.20944/preprints202407.0800.v1

Keywords: Solar hydrogen; Waste Material; Copper slag; Photocatalysis; Metallurgy

Review

Direct Use of Copper Slag as Photocatalytic Material for Solar Hydrogen Production

Susana I. Leiva-Guajardo [1,*], Norman Toro [2], Edward Fuentealba [1], Mauricio J. Morel [3], Álvaro Soliz [4], Carlos Portillo [1] and Felipe M. Galleguillos Madrid [1,*]

[1] Centro de Desarrollo Energético Antofagasta, Universidad de Antofagasta, Antofagasta 1240000, Chile; edward.fuentealba@uantof.cl (E.F.); carlos.portillo@uantof.cl (C.P)
[2] Facultad de Ingeniería y Arquitectura, Universidad Arturo Prat, Iquique 1100000, Chile; notoro@unap.cl
[3] Departamento de Química y Biología, Universidad de Atacama, Av. Copayapu 485, Copiapó 1530000, Chile; mauricio.morel@uda.cl
[4] Departamento de Ingeniería en Metalurgia, Universidad de Atacama, Av. Copayapu 485, Copiapó 1530000, Chile; alvaro.soliz@uda.cl
* Correspondence: susana.leiva.guajardo@ua.cl (S.I.L.G.); felipe.galleguillos.madrid@uantof.cl (F.M.G.M.); Tel.: +56-9-4235-2163

Abstract: Hydrogen has emerged as a promising energy carrier, offering a viable solution to address our current global energy demands. Solar energy stands out as a primary source of renewable power and has the potential to produce hydrogen through the utilization of solar cells. The quest for efficient, durable, and cost-effective photocatalysts is imperative for the advancement of solar-driven hydrogen generation. Copper slag, a by-product stemming from copper smelting and refining processes, primarily consists of metal oxides like hematite, silica, and alumina. This composition renders it a compelling secondary resource for deployment as a photocatalyst, thereby diverting copper slag from landfills. This review aims to comprehensively examine copper slag as a photocatalytic material, exploring its chemical, physical, photocatalytic, and electrochemical properties. Furthermore, it assesses its suitability for water treatment and its potential as an emerging material for large-scale solar hydrogen production.

Keywords: solar hydrogen; waste material; copper slag; photocatalysis; metallurgy

1. Introduction

The rapid expansion of the world´s population and social progress have led to a relentless increase in energy needs in our modern world. This growing demand, fuelled largely by the consumption of fossil fuels, is having a profound impact on our atmosphere, culminating in a worrying increase in the Earth's average temperature [1]. The imperative task of decarbonizing our energy systems is critical to achieving the goals set in 2015. This international agreement, ratified by 196 nations and enacted in 2016, commits to limit global warming to no more than 2°C above pre-industrial levels [2]. In addition, it established the need to reduce greenhouse gas emissions by 40% to 70% between 2010 and 2050 [3].

New energy policies aim to diversify energy sources as a fundamental way to reduce climate change. Solar energy is emerging as a primary source of clean energy, as it represents a fundamental and inexhaustible renewable natural resource. In the last decade, it has emerged as a major contributor to alternative energy solutions.

The solar potential in northern Chile, specifically in the Atacama Desert is 6.23 x 10^8 TWh and is considered a privileged zone worldwide in terms of solar energy. The average direct solar radiation is 2,506 kWh/m^2 per year, higher than that of Spain, Abu Dhabi, and the United States, among other countries [4]. Direct solar radiation in the Atacama Desert reaches approximately 3,000 kWh/m^2 per year [5]. Figure 1 represents the direct solar radiation around the world and expanding the Atacama Desert region.

Preprints.org (www.preprints.org) | NOT PEER-REVIEWED | Posted: 10 July 2024 doi:10.20944/preprints202407.0800.v1

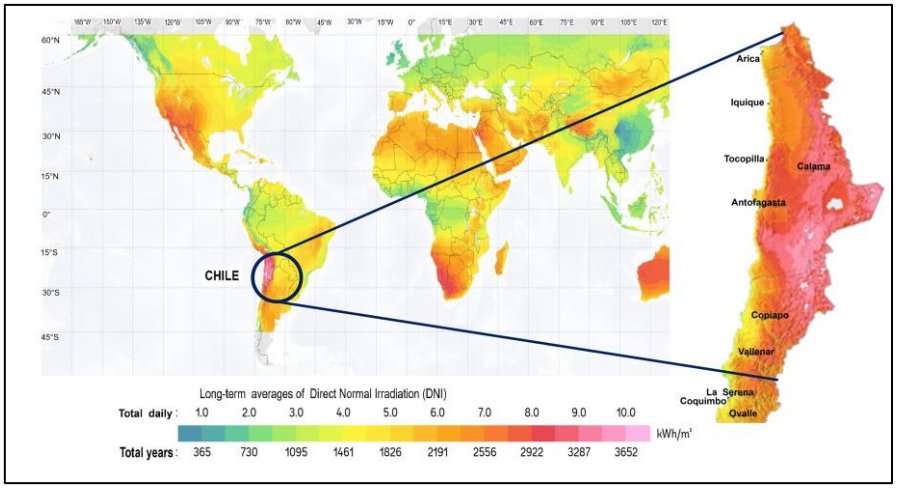

Figure 1. Map of Direct Normal Irradiation in the Atacama Desert, Chile. Modified from Solargis [6].

One of the major obstacles to harnessing solar energy is its intermittent nature. There are several ways to store energy in large quantities in the form of a chemical energy vector, one of which is hydrogen (H_2) [7]. H_2 is a non-toxic fuel with the distinction of being an exceptional clean-burning energy vector, capable of producing up to 120 MJ/kg under standard conditions. This figure far exceeds the energy yield of any fossil fuel [8].

Oreccini et al. consider H_2 as the energy vector of the future and announce it as the protagonist of the "era of energy vectors," which will replace the current "fossil fuel-based economy" [9]. H_2 is often considered the ideal fuel, as it does not produce greenhouse gases during combustion and its main by-product is water. In addition, it has wide applications in producing liquid hydrocarbon fuels and synthetic chemicals. There are several technologies to produce H_2 from fossil fuels, the most common is from natural gas reforming and coal gasification processes. The main drawback of both methods is the imminent emission of CO/CO_2, which contributes to climate change [10]. Solar H_2 generation is one of the most efficient approaches to convert photons into electricity, chemicals, and heat. This achievement is made possible by the synergy of various solar materials, electrochemical devices, and photocatalyst processes [11].

Fujishima et al., indicate that the electrochemical decomposition of H_2O into H_2 and O_2 requires a voltage of 1.23 V between the anode and cathode when using solar panels as the primary energy source or a wavelength of about 1000 nm of solar radiation. In the visible light spectrum, this energy is very effective in an electrochemical system to facilitate the decomposition of H_2O [12]. Fox et al. propose that producing solar H_2 by photocatalysis uses semiconductor materials [13]. Photocatalysis is based on the principle that when a semiconductor is exposed to a light source with the appropriate wavelength, electrons from the valance band pass to the conduction band leaving positive holes in the valence band [14].

Augustynski et al. discussed the key factors that affect the selection of semiconductor materials for solar H_2 production: (i) bandgap energy, (ii) photo corrosion stability, and (iii) flat band potentials [15]. Examples of photocatalytic materials used in solar H_2 production are metal oxides such as titanium dioxide (TiO_2), bismuth vanadate ($BiVO_4$), hematite (Fe_2O_3), and tungsten oxide (WO_3) [11]. Band gap is a crucial parameter to identify the wavelength of light that facilitates the transfer of electrons between energy bands, namely from valence to conduction bands. Table 1 presents the band gap energies and wavelength of semiconductors used in photocatalysis processes.

 doi:10.20944/preprints202407.0800.v1

Table 1. The band gap and wavelength of semiconductors used in photocatalytic processes.

Photocatalyst material	Band gap [eV]	wavelength (nm)	Ref.
ZnO	3.4	365	[16,17]
TiO_2 (anatase)	3.2	380	[18,19]
TiO_2 (rutile)	3.0	414	[19]
Bi_2O_3	2.9	427	[20]
Copper Slag (CS)	2.75	450	[21,22]
Fe_2SiO_4	2.7	---	[22,23]
WO_3	2.7	460	[24]
$BiVO_4$	2.4	---	[16]
CdS	2.4	497	[20,25]
Fe_2O_3	2.3	565	[20,23]
α-Fe_2O_3	1.9	600	[24]
CdSe	1.7	730	[20]

Chen et al, point out that the main disadvantage of TiO_2 and ZnO as photocatalysts lie in their high bandgap energy, see Table 1. These characteristics limit their ability to absorb only ultraviolet light (anatase λ< 390 nm, rutile λ< 414 nm) which represents approximately 4% of the total solar spectrum energy, which restricts their usefulness in practical applications properties [26,27]. They suggest using chalcogenides (ZnS, CdS, and CdSe), which are narrow bandgap semiconductors widely used as photocatalyst properties [28]. Sometimes, it is necessary to generate composite or doped materials to diminish the band gap properties [29]. These narrow bandgap materials allow more efficient absorption of more than 40% of the solar energy in the visible light range, which will eventually improve their photocatalytic properties [30].

Guo et al, indicate that iron oxide (α-Fe_2O_3, hematite) is a promising material for photocatalytic applications due to its narrow band gap of about 2,1 eV, chemical stability, and non-toxicity, which absorbs light up to 600 nm, collects up to 40% of the energy in the solar spectrum and could be one of the cheapest semiconductor materials. In general, sunlight can be divided into three compositions according to wavelength: ultraviolet light (UV, k < 400 nm, E > 3.20 eV, accounts for about 4% of all solar energy), visible light (vis, 400 nm < k < 800 nm, 3.20 > E > 1.60 eV, accounts for about 43%), and near-infrared light (NIR, k > 800 nm, E < 1.60 eV, accounts for about 53%), see Figure 2 [26,31].

Takata et al, in their latest research, aim to develop photocatalysts that can utilize a larger portion of the solar spectrum (longer wavelength) and can stably evolve hydrogen and oxygen gases over several days [21].

 doi:10.20944/preprints202407.0800.v1

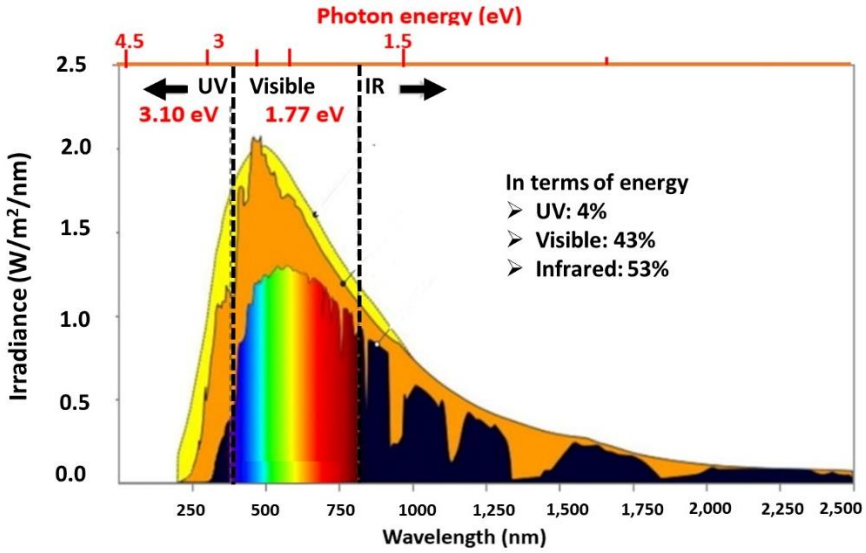

Figure 2. Spectrum of sunlight at sea level. reprinted with permission from ref. [32]. Copyright 2021. Copyright Elsevier.

Huanosta-Gutiérrez et al. in 2012, suggested that it is possible to use copper slag (CS) to catalyze the depletion of pollutants in water sources, therefore, the photocatalytic properties of the material can be thought of [33]. Montoya et al used CS to provide an economically viable method to reduce water pollution and the health impact of industry wastes [22]. The possibility of generating H_2 from toxic alcohols by photocatalytic degradation was evaluated [31].

Since 2012, 8 studies have been published exploring copper slag as a photocatalytic material. Figure 3. These publications have demonstrated the effectiveness of slag in the degradation of organic pollutants, such as industrial dyes, volatile organic compounds, and polycyclic aromatic hydrocarbons [22,33–39]. Only 2 indicate that H_2 production using photocatalysis-assisted solar electrolysis is possible [22,36].

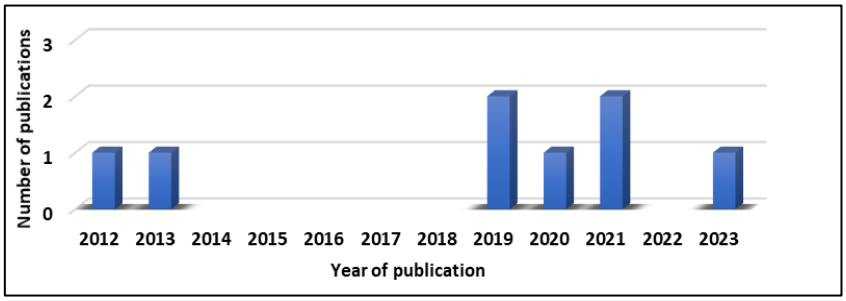

Figure 3. Publication treating photocatalysis and copper slag and contaminant treatment and H_2 production. (source: http://www.scopus.com, 2024, search terms, "hydrogen", and "copper" and "slag", and "photocatalysis" within these results).

The final disposal of CS creates environmental problems worldwide. There is a need to investigate alternative uses for CS as a raw material for other processes. The chemical properties of CSs, rich in iron oxides, are unique and have attracted attention to the production of high-value-added materials for environmental applications, to be used as sorbents, catalysts, or as a source of reactive species in ecological engineering [39]. Several applications for CSs have been found in the last three decades, mainly as a low-cost additive in construction materials [40]. The proposal to use CS as a mining photocatalyst represents a promising avenue as a semiconductor to be used as a photocatalytic material for water treatment and H_2 production.

This manuscript focuses on CS production, characterization techniques, mechanisms and recent advances in photocatalytic reactors for solar H_2 production using nanomaterials. The use of CS charts

 doi:10.20944/preprints202407.0800.v1

a path towards sustainable prosperity for future generations as a clean energy source and its integration into a circular mining economy, fostering more sustainable energy solutions for our planet.

2. Production of Cupper Slag

The smelting process involves separating copper as the main element with a high degree of purity, from contaminants or impurities that reduce its economic value. During copper smelting, five processes are distinguished: (i) flotation, (ii) smelting, (iii) conversion, (iv) fire-refining, and (v) electrolyte-refining cleaning (see Figure 4) [41]. In the Smelting stage, the Cu concentrate (20-30% Cu) composed of bornite (Cu_5FeS_4), chalcopyrite ($CuFeS_4$), pyrite (FeS_2), and chalcocite (Cu_2S), enters the smelting furnace at around 1200°C, releasing gases such as O_2, SO_2, N_2, CO, CO_2, H_2, and $H_2O_{(v)}$. FeO slag and matte (Cu_2S and FeS) have a Cu content between 35– 75%. In the conversion stage, the S and Fe elements present in the sulfide phase are eliminated through an oxidation process, obtaining a relatively pure Cu metal, known as blister Cu (99% Cu). At this stage, the CS is formed while FeO is mixed with Si and $CaCO_3$ to form slag with low Cu content. In the refining stage, the Cu blister obtained from the conversion still contains Ag, Au, As, Sb, Bi, and Fe as impurities. In the last stage, electrorefining processes are used for the recovery of Cu 99.9% purity from Cu concentrate (20-30%Cu). CS usually contains FeO, Fe_3O_4, SiO_2, Al_2O_3, MgO, CaO, and Cu_2O [42].

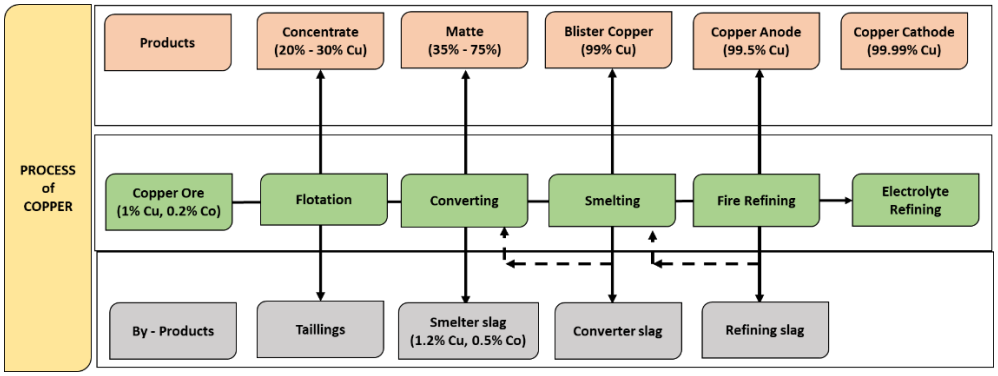

Figure 4. Scheme of Cu slag production, process, product, and by-product. Reprinted with permission from ref. [43]. Copyright 2022. Copyright Elsevier.

2.1. Copper Slag

Cupper Slag (CS) is a residue produced in a pyrometallurgical process to obtain copper concentrated from a concentrate of sulfide minerals, which contains materials such as FeO, SiO_2, Al_2O_3, CaO, and Cu [40]. In the pyrometallurgical stage known as smelting, very high-temperature furnaces are used. As a consequence of the high temperatures, immiscible liquid phases are produced in this process: the copper-rich matte (sulfide) and the CS called oxide [44]. Generally, CS is composed of metallic oxides such as iron oxides (FeO, Fe_3O_4) 30-40%, silicon oxides (SiO_2) 35-40%, aluminium oxides (Al_2O_3 0-10%, and calcium (CaO) 0-10%, which vary their presence in the slag product due to: (i) the nature of the ores, (ii) the nature of the fluxes, (iii) the nature of the concentrates, (iv) the operating conditions, as well as other factors related to the production process [45]. CS is one of the main solid wastes from the pyrometallurgical process applied to the concentrates in the copper industry plants. Chile produces approximately 4.5 million tons of slag per year, and more than 30 million tons of CS are produced annually in the world, which demonstrates the magnitude of the waste from the processing of mining ores. In addition, CS often contains a large amount of valuable metal and is now considered a secondary metal resource [46,47]. These metals can be Fe, Cr, Cu, Al, Zn, Co, Ni, Nb, Ta, and Au and can be recovered by operating units considered in slag ore processing such as (i) crushing, (ii) grinding, (iii) magnetic separation, (iv) flotation, (v) leaching, and (vi) roasting. Cathode materials are becoming increasingly important. Therefore, recycling of metals present in CS can not only recover strategic metals but also contribute to carbon neutrality [48,49]. In

 doi:10.20944/preprints202407.0800.v1

terms of appearance and properties, naturally cooled CSs have a black color, and a glassy surface, dense, lumpy, hard, and brittle (see Table 3). However, depending on the cooling pattern, which can be natural or water-quenched, they can differ in appearance, density, and shape (see Table 4) [50].

Table 3. Physical and mechanical properties of CS [40,51].

Property	Value
Unit weight (T/m^3)	2,8 – 3,8
Absorption	0,13
Bulk density (T/m^3)	2,3 – 2,6
Conductivity (μs/cm)	500
Specific gravity	2,8 – 3,8
Hardness (Moh)	6 – 7
Moisture (ppm)	< 5
Abrasion loss (%)	2,4 – 10
Internal friction angle	40 - 53

Table 4. Visual description of copper smelting slag.

Property	Description	Ref.
Particle shape	Angular	[52–54]
	Irregular	[55,56]
	Multifaceted	[57]
Surface Texture	Glassy	[54,56,58,59].
	Smooth	[50,52,57,59].
	Granular	[60–62]
	Rough	[54]
Color	Black	[54,56,59,63].
	Blackish grey	[57,64].
	Brown with green, red, or black tint	[58,65].

In recent years (1999 -2019), approximately 752 Mt of copper smelting slag have been generated worldwide (see Figure 5), where, the largest generation of this waste occurs in South America (40%), followed by Asia (13%), USA (8%), Oceania (6%), Europe (6%), Africa (6%) and others (15%) [66].

Preprints.org (www.preprints.org) | NOT PEER-REVIEWED | Posted: 10 July 2024 doi:10.20944/preprints202407.0800.v1

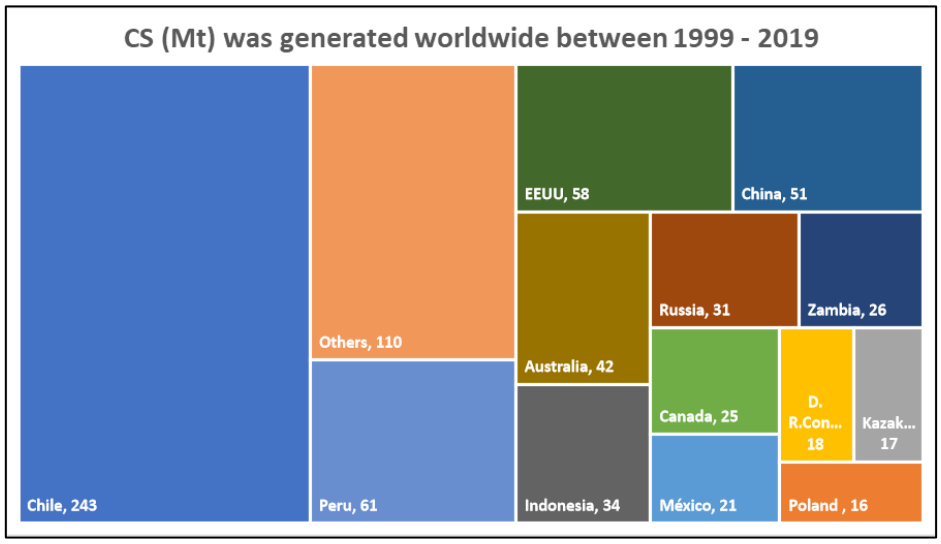

Figure 5. CS (Mt) was generated worldwide between 1999 - 2019 and reprinted with permission from ref. [43]. Copyright 2022. Copyright Elsevier.

There are seven copper smelters in Chile, five of them state-owned and the rest private. Among the state-owned smelters, four are under the jurisdiction of CODELCO: Chuquicamata (Calama), Potrerillos (El Salvador), Ventanas (Puchuncaví), and Caletones (Rancagua), while one operates under ENAMI: the Hernan Videla Lira Smelting Plant (Copiapó). The remaining two smelters, Alto Norte (Xstrata, Antofagasta) and Chagres (Anglo-American, Catemu), are privately owned. Caletones, Potrerillos, and Chuquicamata are switching from slag treatment furnaces to milling and flotation processes. It is worth noting that between 1999 and 2019, Chile accounted for approximately one-third of the world´s production of copper smelting slag. This is equivalent to an average annual production of 12 million tons, coming from the seven existing copper smelters in the country [46]. The location, capacity, and production of the Chilean smelters are reported in Figure 6.

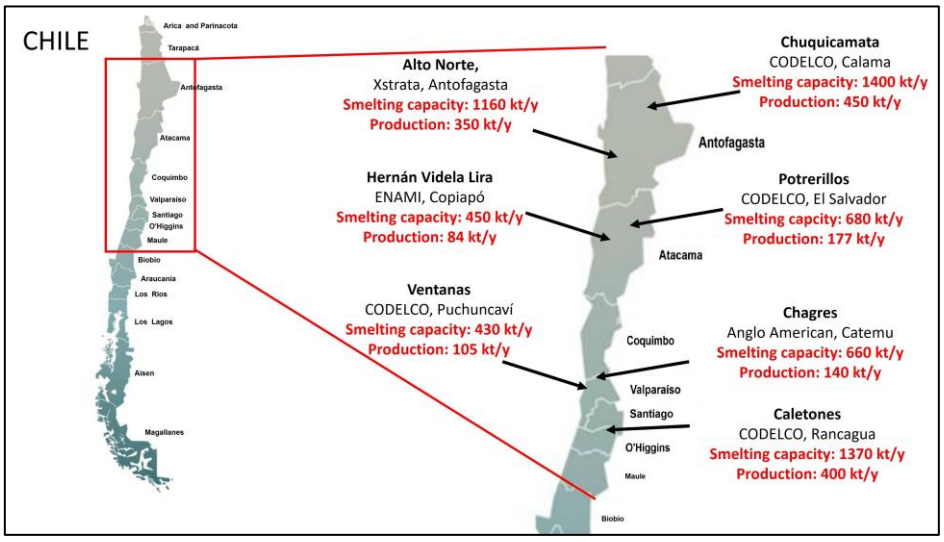

Figure 6. Location, capacity, and production of the Chilean smelters.

The photocatalytic application of CS has recently been studied [22]. The nanometric use of CS in a natural way enables the change of the photocatalytic activity from UV wavelengths to sunlight, which allows looking at this waste as a semiconductor that can be used as a great contribution to the environment.

 doi:10.20944/preprints202407.0800.v1

3. Chemical and Superficial Characterization of Cupper Slag

Several established techniques can be used for the comprehensive characterization of CS, such as (i) optical microscopy, (ii) scanning electron microscopy (SEM), (iii) electron microprobe analysis (EMPA), (iv) X-ray diffraction (XRD), (v) X-ray fluorescence spectroscopy (XRF), and (vi) Raman spectroscopy. These methods provide valuable information on the phase composition of the material and the spatial distribution of metallic elements in the different phases. The integration of all these analytical approaches allows a comprehensive characterization of the CS, covering its chemical composition and mineralogical properties [40].

The chemical characterization of CS allows for identifying the compounds present in them by X-ray fluorescence (XRF) [67]. The crystalline phases of CS are generally composed of fayalite (Fe_2SiO_4), magnetite (Fe_3O_4), quartz (SiO_2), and some iron and copper sulfides. The predominant elements contained in CS are Fe and Si [68]. Phiri et al, this study delved into the feasibility of incorporating CS as a valuable resource within the framework of the circular economy. The researchers meticulously compiled data on the average chemical composition of these waste materials from a comprehensive review of 80 previous studies conducted in 21 countries. These include Chile, Canada, Australia, China, Democratic Republic of Congo, Finland, Italy, Iran, Kazakhstan, Namibia, Mexico, Serbia, Poland, Singapore, South Africa, South Korea, Spain, Turkey, the United States and Zambia, (see Table 7)

Table 7. Average chemical composition of copper smelting slags for major and minor elements in 21 countries. Reprinted with permission from ref. [43,69]. Copyright 2021. Copyright Elsevier.

Components	SiO_2	FeO	Fe_2O_3	CaO	Al_2O_3	MgO	K_2O	S	MnO	TiO_2	P_2O_5	Na_2O
(wt%)	33,18	32,15	31,93	6,21	5,88	2,02	1,53	1,19	0,42	0,40	0,39	0,06

Elements	Ca	Al	Zn	Ag	Mg	Cu	Pb	Co	As	Ti	Ni	Mn	Sb	Mo
(wt%)	3,05	2,59	1,83	1,67	1,36	1,19	0,94	0,48	0,38	0,28	0,24	0,22	0,10	0,06

X-ray diffraction (XRD) analysis determines the crystalline phases present and, in general, allows identifying and obtaining the relative abundance, i.e., estimating the amorphous percentage of the sample.[69] For example, Figure 6 shows the crystalline phases of fayalite (Fe_2SiO_4), and magnetite (Fe_3O_4), Figure 7.

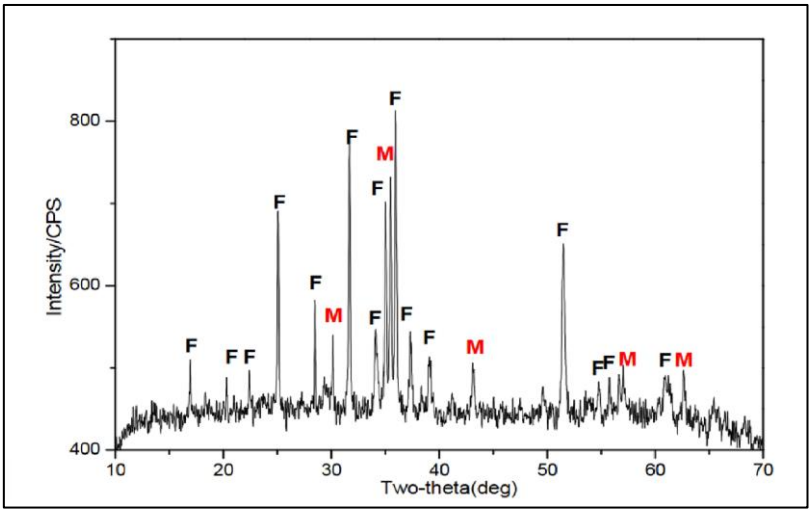

 doi:10.20944/preprints202407.0800.v1

Figure 7. X-ray diffraction patterns of CS (F- fayalite; M-Magnetite). Reprinted from ref. [70].

Scanning electron microscopy (SEM) is a valuable tool that provides structural information to evaluate very small surface topographic details of whole objects or powders, due to its higher resolution [71]. Figure 8, presents the micrographs of the CS from Tongling, China, it is observed that fayalite and magnetite are the main minerals in CS, and they are closely combined with copper matte and the glassy phase, Figure 8.

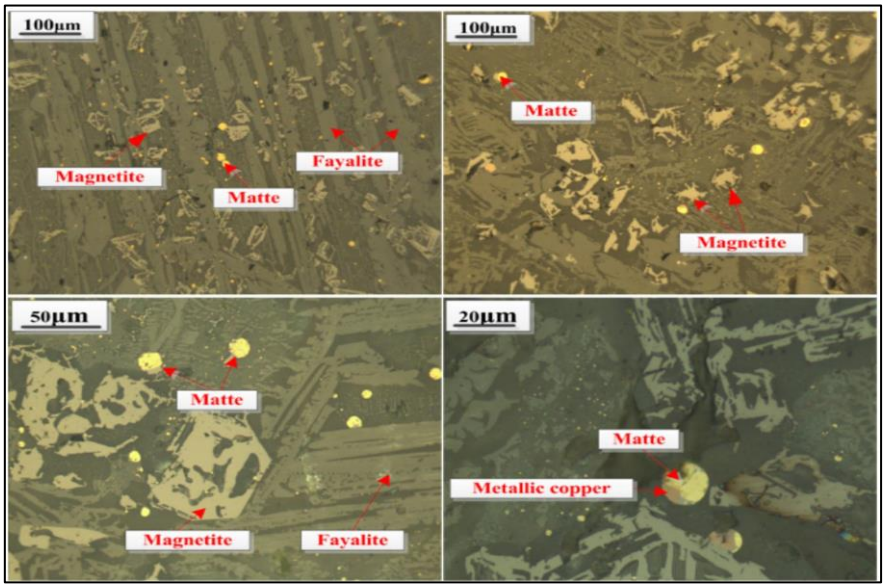

Figure 8. Microstructure of CS, Tongling, China. Reprinted from ref. [70].

Many researchers use SEM and DRX images to identify the surfaces' morphological characteristics, the material's crystalline structure, and their chemical composition [37,38,43,44,51,52,58,61,62,70,72–88]. The presence of metal oxides such as iron oxide and copper oxide in the slag serves as active sites to promote photocatalytic reactions. Therefore, reusing CS as a photocatalyst is an opportunity to contribute to environmental sustainability and envisions an opportunity for H_2 generation.

4. Semiconductor Electrodes as Photocatalysts

Lasia et al. explain that in the presence of a conductive electrode, either metallic or glassy carbon, in contact with an electrolytic solution, an excess of electronic charge accumulates on the electrode surface, resulting in charge distribution mainly within the solution. In the case of semiconductor electrodes, the concentration of conductive species (electrons or holes) is significantly lower than that of the surrounding solution. Consequently, a redistribution of space charge occurs within the semiconductor electrode. Depending on how the charge is distributed within the conduction and valence bands, a potential bending occurs at the surface. In the case of an open-circuited n-type semiconductor electrode, this bending is directed upwards from the band edges. In contrast, p-type semiconductors exhibit a bending downward from the band edges [89,90]. Tanaka et al. investigated TiO_2 passive oxide film which exhibits excellent semiconductor characteristics.

Montoya-Bautista et al. evaluated CS using electrochemical techniques to measure its properties as a photocatalyst and demonstrated the electrochemical and photoelectrochemical behavior using the Mott-Schottky model. Five different values of frequency (100 – 1000 Hz), detecting the presence of two semiconductors in the CS such as fayalite, and magnetite. The lower part of the conduction band (CB) must have a potential more negative than the reduction potential of H^+ to H_2 (0,41 V v/s NHE).

Likewise, the upper part of the valence band (VB) must exceed the oxidation potential of H_2O to O_2 (0,82 V v/s NHE). Therefore, the bandgap energy (Eg) of the photocatalysts must be at least 1.23

 doi:10.20944/preprints202407.0800.v1

eV to achieve water-splitting [91]. Figure 9, represents a schematic band diagram of the photocatalytic performance of semiconductors, (a) of type n and (b) of type p. The orange horizontal range indicates the redox potentials of OER and HER, and the purple dashed horizontal lines indicate the redox potential, respectively [92–94].

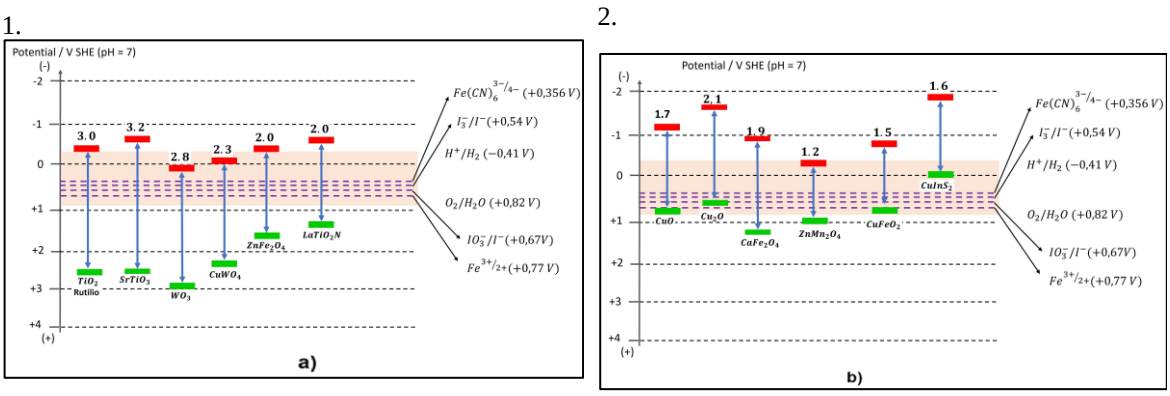

Figure 9. Schematic diagram of some semiconductors a) type n and b) type p. Reprinted from ref. [92].

In Figure 9, it is observed that the conduction bands of fayalite are above the redox potential for H_2 production [92]. The photogenerated holes residing in the valence band of fayalite exhibit the ability to degrade alcohol efficiently. This ability stems from the fact that the valence band potential of the fayalite falls below the redox oxidation potential of the alcohol, thus satisfying the essential thermodynamic criteria for the concurrent reduction of water constituents and oxidation of alcohols [22,95].

Figure 10, represents the band gap diagram and other semiconductors that can be used for solar H_2 production.

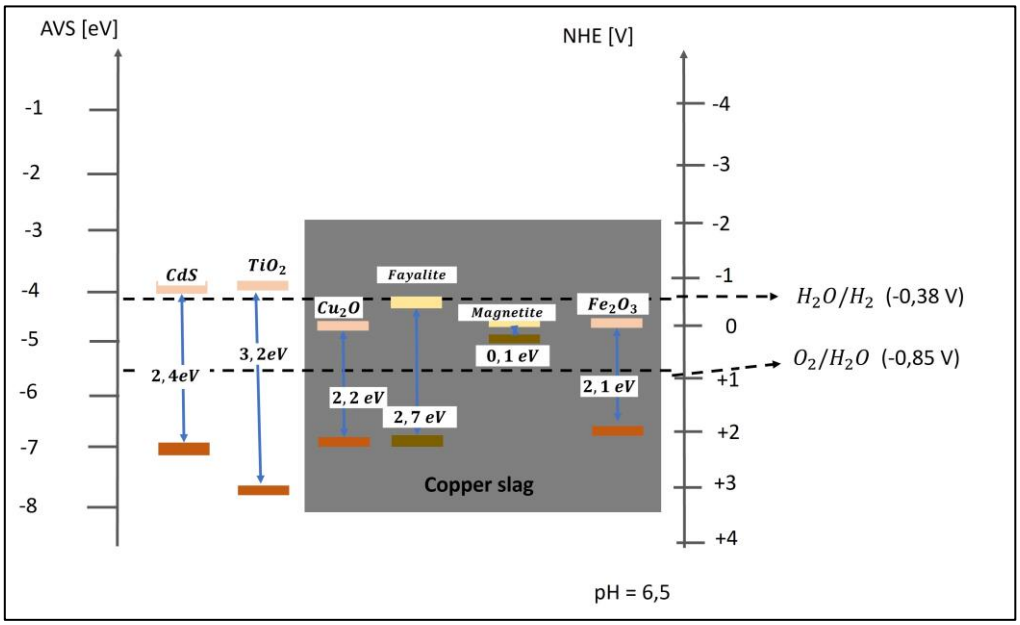

Figure 10. Bandgap diagram for CS and other semiconductors at pH=6,5. The low bands, in a dark color, are the valence bands (VB), and the high bands, in light color, are the conduction bands (CB), and in the center the band gap values. Mineralization is possible if the potential is within the band gap (AVS: absolute vacuum standard). Reprinted with permission from ref. [22]. Copyright 2020. Copyright Springer Nature.

 doi:10.20944/preprints202407.0800.v1

Montoya-Bautista et al. used CS as a photocatalytic material. The test was performed using different electrolytes such as methanol, isoamyl alcohol, and propanol. The main objective was to evaluate the efficiency of these compounds in the generation of H_2 by a photocatalytic process. In particular, H_2 production showed higher rates when subjected to simulated solar irradiation compared to mercury irradiation. These results highlight the importance of both the type of compound and the light source in influencing H_2 production by photocatalysis [22].

The use of industrial by-products or waste materials as photocatalysts has emerged as a promising approach to curb the production costs associated with titanium semiconductor-based materials. Among these by-products, crude or modified metallurgical slags are a viable option due to their cost-effectiveness, wide availability, and favorable optical properties. Numerous investigations have shown that both steel and blast furnace slag are capable of removing chemical contaminants, degrading dyes, and even producing H_2 under simulated solar irradiation [38,96,97]. Because the other components of the slag could interfere with the photocatalytic mechanism of CS, it is necessary to know the photocatalytic properties of solar photocatalysis of CS, including bandgap engineering and surface modification, is essential to improve its catalytic activity and stability.

4.1. CS as Photocatalytic Material

CS exhibits distinctive chemical attributes, particularly its valuable photocatalytic properties used for the solar-driven oxidation of organic pollutants in industrial wastewater and H_2 production.

Solis-López et al, realized that the general use of CS is in cement concrete, and little research has been conducted to evaluate this material as a catalyst [39]. But Montoya et al, in their investigations, indicated that the use of CS as a Fenton-type photocatalyst is both an innovative alternative for the reuse of these wastes and an environmentally friendly option. Also, it indicates that the studied CS material acts as an n-type semiconductor with a band-gap of 2.75 eV, with absorption energy mainly in the violet-green range of the visible spectrum [22].

Zhang et al. studied a nanomaterial based on alkali-activated blast furnace slag as a new catalyst for H_2 production. They concluded that this slag-based synthesized nanomaterial has a mesoporous structure whose main characteristics are (i) it has a large specific surface area, (ii) uniform pores, (iii) high ion-interaction ability, and (iv) the relative ease of synthesis [96]. In addition, they activated blast furnace slag using alkali, which led to the creation of a new catalyst for H_2 production. In this context, semiconductors such as Fe_2O_3 and TiO_2 assume crucial roles as active catalyst materials. Consequently, this alkali-activated blast furnace slag-based nanomaterial emerges as a highly efficient H_2 producer due to the synergistic interaction between the oxide and its alkaline properties. [96] Figure 11, shows the H_2 production scheme in the alkali-activated granulated blast furnace slag catalyst by photocatalytic water-splitting [24,77,91,98].

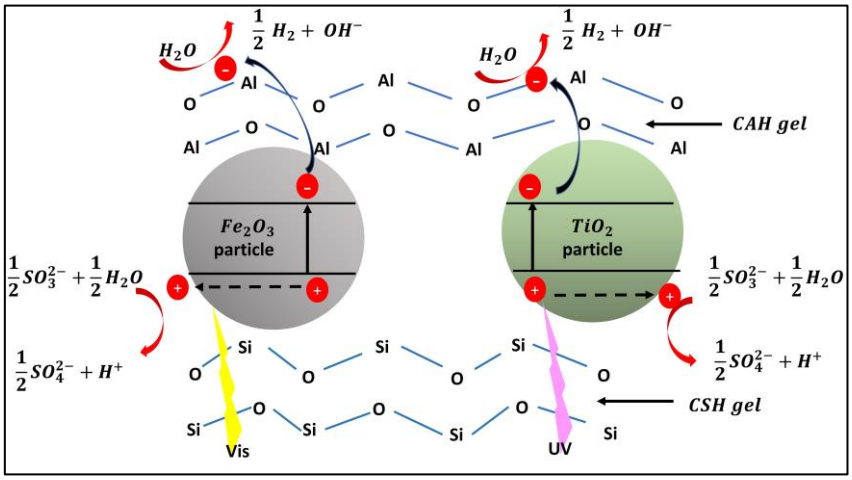

Figure 11. Schematic representation of the production of H_2 on the granulated blast furnace slag catalyst activated with alkali by photocatalytic decomposition of water. Reprinted with permission from ref. [96]. Copyright 2014. Copyright Elsevier.

 doi:10.20944/preprints202407.0800.v1

Zhang et al. investigated a cementitious material comprised of granulated blast furnace slag activated with alkali, which catalyzed the photocatalytic decomposition of water to synthesize H_2 [96]. Montoya-Bautista et al. demonstrated the band edges of the fayalite and magnetite in the CS [22]. It is observed that the conduction bands of the fayalite are above the redox potential for the production of H_2 [99]. The photogenerated holes residing in the valence band of fayalite exhibit the capacity to degrade alcohol efficiently. This capability stems from the fact that the valence band potential of fayalite falls below the redox oxidation potential of alcohol, thereby satisfying the essential thermodynamic criteria for the concurrent reduction of water constituents and oxidation of alcohols.

Arzate-Salgado et al, conducted a study evaluating the effectiveness of copper slag as a Fenton-type photocatalyst. They found that copper slag, when in an acidic medium with the presence of hydrogen peroxide and exposed to simulated sunlight, successfully degraded diclofenac [100]. On the other hand, Huanosta-Gutiérrez et al and Solís-López, demonstrated that copper slag also has a high photocatalytic activity in the photo-Fenton process, both in an acidic medium and combined with hydrogen peroxide and UV radiation or simulated sunlight [33,39].

Mercado-Borrayo et al, indicate that the band gap of fayalite, the majority phase of copper slag, is 2.5 +/- 0.1 eV, making it capable of absorbing the blue-green part of the visible spectrum. This allows sunlight to be used as an energy source for photocatalysis instead of relying primarily on UV radiation [82]. García-Estrada et al. demonstrate the high efficiency and stability of metallurgical copper slag (CS) as a heterogeneous Fenton-type catalyst for the degradation of trace thiabendazole in different contaminated aqueous matrices, using the CS-H_2O_2 system at circumneutral pH under natural solar irradiation NSI [35,37].

4.2. Photocatalytic Mechanisms Applied to CS.

Zhang et al, show the photocatalytic mechanism of alkali-activated slag, reactions 1 to 4. Reaction 3, indicates the action of sacrificial reagent, which promotes the formation of SO_4^{2-}, and H^+, respectively [96].

$$Fe_2O_3 \xrightarrow{h\nu} Fe_2O_3\,(h^+) + e^- \quad (1)$$

$$TiO_2 \xrightarrow{h\nu} TiO_2\,(h^+) + e^- \quad (2)$$

$$H_2O + e^- \rightarrow \tfrac{1}{2}\,H_2 + 0H^- \quad (3)$$

$$\tfrac{1}{2}\,H_2O + \tfrac{1}{2}\,SO_3^{2-} \rightarrow \tfrac{1}{2}\,SO_4^{2-} + H^+ \quad (4)$$

Morales-Perez et al, propose a Langmuir-Hinshelwood type mechanism with a single dual site type, in which water molecules and an acidic solution are adsorbed (ads) on the surface of the CS (CS), in turn, when the CS is irradiated ($h\upsilon$), it generates the charge pair, the hole in the valence band (VB) and the electron in the conduction band (CB). The adsorbed water (ads) interacting with the hole generates the hydroxyl radical and an adsorbed proton. On the other hand, the degradation of acid solution (acting as a sacrificial agent) occurs using the produced hydroxyl radicals or the photogenerated holes producing other acids, methane, and carbon dioxide as main products. Desorption of the products regenerates the surface sites. H_2 is produced by proton reaction using photogenerated electrons in the conduction band of CS [36].

Montoya-Bautista et al. interpreted that the sacrificial agent acts as a scavenger, favoring the reduction of H_2O by reacting with the h+ species or $*OH_{ads}$ generated on the CS surface, avoiding recombining the e-/h+ pair. The representation of the reactions 5 and 6 is as follows:

 doi:10.20944/preprints202407.0800.v1

$$H_2O + h^+ \rightarrow OH^- + H^+ \quad (5)$$

$$2H^+ + 2e^- \rightarrow H_2 \quad (6)$$

The hydroxyl radicals produced in Equation 5, are captured during the degradation of the sacrificial agent. The H_2 production is related to the number of electron/hole pairs formed during irradiation. In addition, the semiconductor used, CS, is n-type, so Equation 6, can be depleted due to the adsorption of H^+ on the negatively charged catalyst surface [99]. The low H_2 production is limited because the electrons required are scattered over a large area, and the H^+ remains attached to the catalyst surface after it has lost its hydroxyl groups.

Solis-López et al, mention that magnetite is a more efficient catalyst than hematite for heterogeneous Fenton reactions because magnetite has a combination of Fe^{2+} and Fe^{3+} oxidation states. The combination of 2+ and 3+ oxidation states in magnetite increases the rate of -OH radical production because the reaction rate of H_2O_2 with $\equiv Fe^{2+}$ sites is significantly higher than the rate with $\equiv Fe^{3+}$ sites [39].

Garcia-Estrada et al, evaluated the catalytic ability of metallurgical copper slag (CS) for pesticide removal in real wastewater by the heterogeneous photo-Fenton process at circumneutral pH under natural solar irradiation (NSI) [35].

The photo-photon reaction indicates that the active sites ($\equiv Fe^{3+}$ - OH) adsorb H_2O_2 on the iron oxide surface and form a complex, reaction 7:

$$\equiv Fe^{3+}\text{-}OH + H_2O_2 \rightleftarrows (H_2O_2)_s \quad (7)$$

Electron transfer then occurs and $\equiv Fe^{2+}$ and HO^{2-} peroxyl hydroxyl radicals are formed, reaction 8 and 9:

$$(H_2O_2)_s \rightleftarrows (\equiv Fe^{2+}O_2H) + H_2O \quad (8)$$

$$\equiv Fe^{2+}O_2H) \rightleftarrows \equiv Fe^{2+} + HO_2^{\bullet} \quad (9)$$

Subsequently, $\equiv Fe^{2+}$ catalyzes the decomposition of H_2O_2 into HO^- radicals, reaction 10:

$$H_2O_2 + \equiv Fe^{2+} \rightleftarrows \equiv Fe^{3+}\text{-}OH + HO^{\bullet} \quad (10)$$

At the same time, oxidation of $\equiv Fe^{2+}$ to $\equiv Fe^{3+}$ occurs in the presence of oxygen and by peroxyl and peroxyl hydroxyl radicals, reactions 11 and 12:

$$\equiv Fe^{2+} + O_2 \rightleftarrows \equiv Fe^{3+}\text{-}OH + HO_2^{\bullet} \quad (11)$$

$$\equiv Fe^{3+}\text{-}OH + HO_2^{\bullet}/O_2^{\bullet-} \rightleftarrows \equiv Fe^{2+} + H_2O/OH^- + O_2 \quad (12)$$

They demonstrated that the CS-H_2O_2-NSI system produced hydroxyl radicals (OH^-) [35].

Using CS as a photocatalyst opens interesting perspectives for the efficient and cost-effective production of H_2. Optimizing the photocatalytic properties of solar photocatalysis of CS, including the study of band gap and surface modification, is essential to improve its catalytic activity and stability. In the following, several efficient reactor designs and photocatalytic systems are proposed that can improve H_2 production rates and conversion efficiencies.

4.3. Photocatalytic Reactors for H_2 Production

Focusing on the prospects for a green H_2 economy, a photocatalytic device is proposed that uses solar energy to split water and produce H_2. Since both reactions require significant amounts of kinetic

Preprints.org (www.preprints.org) | NOT PEER-REVIEWED | Posted: 10 July 2024 doi:10.20944/preprints202407.0800.v1

overpotentials, a practical photocatalyst would need to have a band gap energy in the range of 1.6 – 2.4 eV to drive overall water-splitting [101].

Fujishima et al. observed the photosynthesis phenomenon using an electrochemical system with n-type TiO_2 semiconductor electrodes. They demonstrated the possibility of using a solar photocatalyst for photosynthesis. They use a solar-powered titanium electrolyzer to split water and produce H_2 as fuel [18].

Lo et al., developed an innovative dual-chamber reactor to isolate the production of hydrogen and oxygen in the photocatalytic splitting of water with visible light. See Figure 12. They used a modified Nafion membrane that divides the reactor so that hydrogen and oxygen evolve separately. They used Z-scheme catalysts, $Pt/SrTiO_3$:Rh and WO_3, as hydrogen photocatalyst and oxygen photocatalyst, respectively. In addition, Fe^{2+} and Fe^{3+} were added as electron transfer mediators [102].

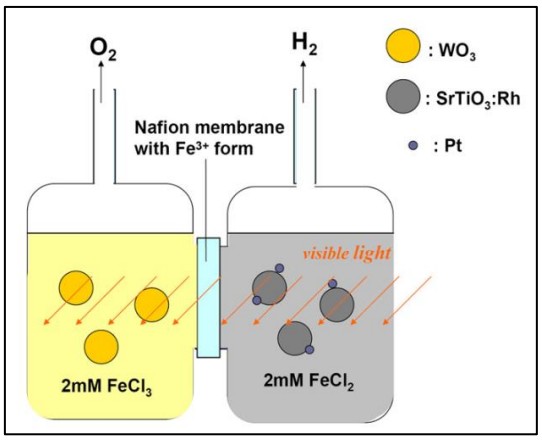

Figure 12. Schematic diagram of the dual-chamber reactor system [102].

In 2012, Dincer et al, comprehensively outlined sustainable and environmentally friendly methods for H_2 production, classifying them according to their driving sources and applications [103].

Borges et al. conducted a study on solar photocatalysis using a continuous fixed-bed reactor configuration. This configuration comprises a glass cylinder placed in the core of a parabolic solar collector, inside which the photocatalytic material is packed—in this case, volcanic sand serves as the photocatalytic material. The objective is to circulate the contaminated solution through the fixed-bed reactor, as depicted in Figure 13. This photoreactor presented by Borges et al, achieves a greater contact between the photocatalyst and the dissolution of pollutants, and better H_2 production, resulting in more scalable equipment from the industrial point of view [104].

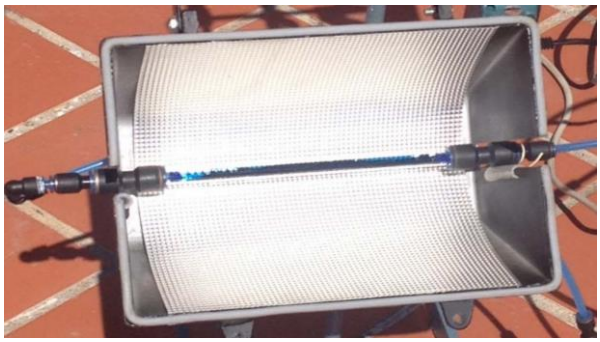

Figure 13. Photocatalytic cell fixed bed packing, Reprinted from ref. [104].

Herrera-Ibarra et al. investigated for the first time the application of CS in the treatment of wastewater from a textile industry using the solar heterogeneous solar photo-Feton process (due to the use of Fe material) under solar irradiation. See Figure 14. For the experiments the first thing they did was to adjust the pH of the wastewater by acidifying it, then they placed the reactor under natural

 doi:10.20944/preprints202407.0800.v1

sunlight and the CS was deposited on the bottom of the reactors, distributing it evenly. Wastewater is added to each reactor and also 30% H_2O_2. Finally, the water mixture is recirculated at a constant flow rate. CS and exposure to sunlight did not contribute to water toxicity. Herrera et al., only refer to water treatment, H_2 production remains to be investigated [37].

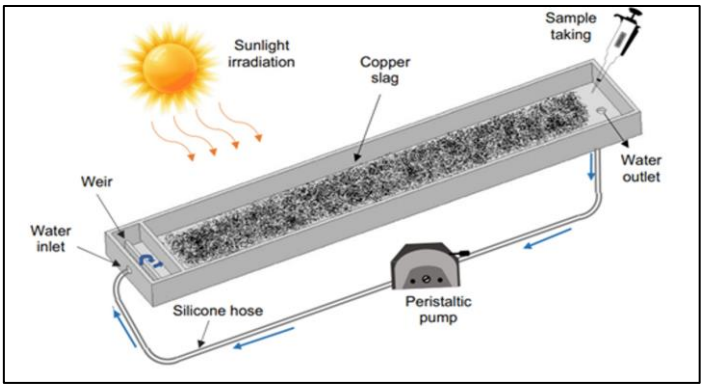

Figure 14. Heterogeneous photocatalytic treatment of water can be bifunctional if H_2 is produced during the degradation of pollutants Reprinted with permission from ref. [37]. Copyright 2022. Copyright Springer Nature.

Li et al. developed an optofluidic microreactor with staggered micropillars in the microreaction chamber. See Figure 15. They enlarged the surface area for loading the photocatalyst and induced turbulence in the fluid flow, increasing the mass transfer to boost the hydrogen production rate [105].

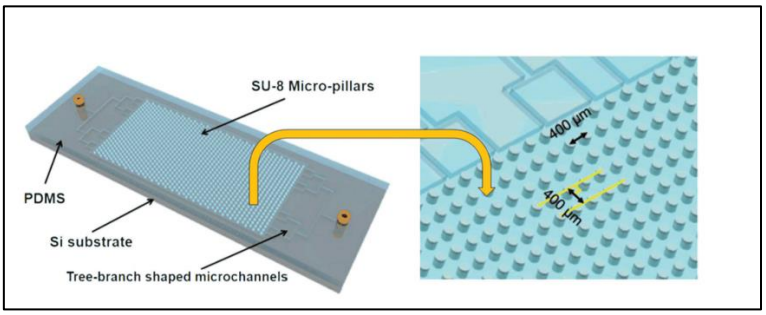

Figure 15. (a) Schematic of the high surface area optofluidic microreactor with micro-pillar structure. (b) Cross section of the staggered micro-pillars in the reaction chamber [105].

Kim et al. propose that water-splitting is a promising method for converting sunlight into renewable, sustainable, and environmentally friendly H_2 energy. Photovoltaic-assisted electrochemical, photoelectrochemical, and photocatalytic water-splitting systems can generate solar H_2 from water [101]. The reactor design for producing solar H_2 by photocatalytic decomposition of water is a plate reactor using photocatalytic films, Figure 16. The photocatalytic reactor comprises a UV-transparent glass window and a photocatalyst sheet ($SrTiO_2$/Al). The polyurethane pipe is used to transport gaseous products and reactive water [106].

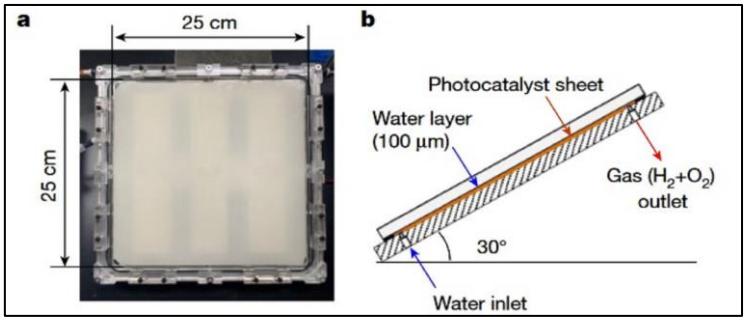

 doi:10.20944/preprints202407.0800.v1

Figure 16. a. Photographic image of a panel reactor unit. b. The structure of the panel reactor unit is viewed from the side Reprinted with permission from ref. [106]. Copyright 2021. Copyright Springer Nature.

The photocatalytic reactor presents low solar to H_2 (STH) conversion efficiencies values of around 1 – 8%, but the design of these systems is much simpler, and inexpensive improvements in photocatalysts performance could make these systems viable and allow to taking advantage of their simplicity and scalability [106]. The photocatalytic reactors play a crucial role in solar hydrogen production, enabling efficient solar energy conversion into clean, sustainable, and storable hydrogen. They play an important role in transitioning to a cleaner, more sustainable energy economy. These reactors use sunlight to activate a photoactive semiconductor, such as titanium dioxide (TiO_2), which acts as a catalyst to split water into hydrogen and oxygen. These reactors can efficiently harness solar energy and convert it into hydrogen.

The use of CS as a photocatalytic semiconductor will help reduce the demand for virgin materials, reducing the need for new extraction processes and reducing the amount of waste generated in the mining industry.

5. Discussion

Chile is a country with an enormous metallurgical tradition, a productive activity that has had an important development from the mid-19th century to the present day. Bibliographic antecedents describe that in the north of Chile, particularly in the regions of Coquimbo and Atacama, numerous smelters were established near the copper mining deposits, registering 146 copper smelters with a total of 347 furnaces in 1858 (National Mining Society, 1894). These smelters generated CS, which has remained in landfills as abandoned deposits ever since, causing effects on the landscape, soil, and water, as an economic, and social impact [58].

The direct use of CSs as a photocatalytic material for solar H_2 production is an interesting and promising research topic. The use of CS as a photocatalyst for H_2 production presents a remarkable opportunity for both waste recovery and sustainable energy generation. With the significant volume of slag generated by the global copper industry, one of its main advantages lies in its abundant availability. Reuse of this can reduce environmental pollution and optimize resource efficiency. The exceptional photocatalytic performance of CS can be attributed to its specific chemical composition and distinctive surface properties. In particular, its broad surface area enhances reagent adsorption and catalytic activity. In addition, the presence of metal oxides such as iron oxide and copper oxide in the slag serves as active sites to promote photocatalytic reactions.

Montoya-Bautista et al, conducted photocatalytic studies on CSs. These are the first studies that were carried out in 2021. It indicates that the nanometric use of CS in a natural way allows the change of photocatalytic activity from UV wavelengths to sunlight, which allows contemplating this waste as a semiconductor that can be used as a great contribution to water treatment and proposes that it is necessary to study the production of H_2 by photocatalysis [22]. The use of CS as a photocatalyst opens up interesting prospects for the efficient and cost-effective production of H_2. However, this field of research presents many challenges and considerations. First, optimization of the photocatalytic properties of copper solar photocatalysis, including bandgap engineering and surface modification, is critical to improve its catalytic activity and stability. In addition, the development of efficient reactor designs and photocatalytic systems is crucial to maximize H_2 production rates and conversion efficiency.

It is proposed to improve methodology, for example: The presence of metal oxides such as iron oxide and copper oxide in the slag serve as active sites to promote photocatalytic reactions. Therefore, reusing CS as a photocatalyst is an opportunity to contribute to environmental sustainability and envisions an opportunity for H_2 generation. To answer what are the limitations of using CS as a photocatalytic material it is necessary to study the individual characteristics of the material components. Therefore, it is proposed to study the morphologies of the material, in powder form, as slag and its components. Which wavelength predominates, to see which sector of the solar spectrum

 doi:10.20944/preprints202407.0800.v1

it covers? Perform replications and provide additional details on the procedures and methods used. This is to facilitate replication of the study by other researchers and to contribute to consistent and reliable results. Furthermore, it is imperative to evaluate the environmental footprint and potential toxicity linked to the employment of CS as a photocatalyst. Thorough characterization and risk assessment studies are essential to ensure the safety and sustainability of the process. The direct utilization of Cu dross as a photocatalytic material for H_2 production via solar energy holds significant promise in the realm of renewable energy. Nonetheless, additional research and development endeavors are warranted to fully explore the extent of its functionality and applicability. These efforts will, in turn, make a substantial contribution towards shaping a cleaner and more sustainable energy landscape for the future.

So far, most of the published work has been empirical and focused on acidic conditions to remove the contaminant. In addition, the amount of H_2 produced has not been determined. However, it is an opportunity to conduct studies on the behavior of CS under saline conditions for H_2 production.

6. Conclusions

The direct use of CS as a photocatalytic material for solar H_2 production in locations with high solar radiation highlights its potential as a sustainable and cost-effective solution. These are the key conclusions drawn from the review, (i) the valorization of CS as a byproduct of copper extraction and refining processes, offers an opportunity to generate other business for CS. CS as a photocatalyst contributes to environmental sustainability. (ii) CS is abundantly available due to the significant quantities generated by the copper industry worldwide. Its use as a photocatalyst maximizes resource efficiency and reduces waste. (iii) CS has a unique chemical composition and surface characteristics that make it suitable for photocatalytic reactions. Its high surface area and the presence of metal oxides contribute to its photocatalytic activity. (iv) the direct use of CS as a photocatalytic material enables solar H_2 production and offers a sustainable pathway to produce clean fuel. By harnessing solar energy, this approach takes advantage of the abundant sunlight in many arid parts of the world. (v) optimization of photocatalytic properties, reactor design, and environmental impact assessment are crucial aspects to be addressed in future research.

Due to the presence of other elements in the CS, there will be obstacles in the mechanism of the photocatalysis of the CS. Therefore, it is crucial to have a detailed knowledge of factors such as chemical composition, structure and crystallinity, surface states, morphology, and electrical properties to determine the photocatalytic activity of CS. Studies show that CS is a chemically stable and efficient Fenton-type catalyst for the degradation of micropollutants in wastewater.

Overall, the review highlights the potential of using CS as a photocatalytic material for solar H_2 production. Further research and development efforts are needed to optimize its properties, design efficient systems, and evaluate the environmental implications. By exploring and overcoming these challenges, the direct use of CSs can contribute to a more sustainable and cleaner energy future.

Author Contributions: Conceptualization, S.L.G. and F.M.G.M.; methodology, S.LG. and F.M.G.M.; validation, A.S., E.F., C.P. M.J.M. and N.T.; investigation, S.LG., N.T. M.J.M. and F.M.G.M.; writing—original draft preparation, S.LG., E.F., N.T. and F.M.G.M.; writing—review and editing, S.LG., E.F., M.J.M, A.S., C.P, N.T. and F.M.G.M.; visualization S.L.G., A.S., and F.M.G.M.; supervision, F.M.G.M. All authors have read and agreed to the published version of the manuscript.

Funding: This research received no external funding.

Acknowledgments: The authors would like to thank the Programa de Doctorado en Energía Solar of the Universidad de Antofagasta, Chile. The authors are grateful for the support of ANID-Chile through the research projects FONDECYT Iniciación 11230550 and ANID/ FONDAP 1522A0006 Solar Energy Research Center SERC-Chile.

Conflicts of Interest: The authors declare no conflicts of interest.

References

1. S. Nasirov, A. Girard, C. Peña, F. Salazar, and F. Simon, "Expansion of renewable energy in Chile: Analysis of the effects on employment," *Energy*, vol. 226, p. 120410, Jul. 2021, doi: 10.1016/j.energy.2021.120410.
2. P. Del Río and C. P. Kiefer, "What will be the cost of renewable electricity generation technologies in the future?," *papers of the*, pp. 34–250, 2022.
3. G. Peñaranda, P. C. Vanegas, and M. Castañeda, "Carbon footprint calculation: Review key elements for the development of an opertional tool," *Seeds of knowledge magazine*, vol. 2, no. 1, pp. 60–65, 2022.
4. C. Moraga-Contreras *et al.*, "Evolution of Solar Energy in Chile: Residential Opportunities in Arica and Parinacota," *Energies (Basel)*, vol. 15, no. 2, Jan. 2022, doi: 10.3390/en15020551.
5. C. Parrado, A. Girard, F. Simon, and E. Fuentealba, "2050 LCOE (Levelized Cost of Energy) projection for a hybrid PV (photovoltaic)-CSP (concentrated solar power) plant in the Atacama Desert, Chile," *Energy*, vol. 94, pp. 422–430, Jan. 2016, doi: 10.1016/j.energy.2015.11.015.
6. Solargis, "Solar resource maps of World. © 2020 The World Bank, Source: Global Solar Atlas 2.0, Solar resource data: Solargis.," © 2020 The World Bank, Source: Global Solar Atlas 2.0, Solar resource data: Solargis.
7. R. Van De Krol, Y. Liang, and J. Schoonman, "Solar hydrogen production with nanostructured metal oxides," *J Mater Chem*, vol. 18, no. 20, pp. 2311–2320, 2008, doi: 10.1039/b718969a.
8. M. K. T. Chee, B. J. Ng, Y. H. Chew, W. S. Chang, and S. P. Chai, "Photocatalytic Hydrogen Evolution from Artificial Seawater Splitting over Amorphous Carbon Nitride: Optimization and Process Parameters Study via Response Surface Modeling," *Materials*, vol. 15, no. 14, Jul. 2022, doi: 10.3390/ma15144894.
9. F. Orecchini, "The era of energy vectors," *Int J Hydrogen Energy*, vol. 31, no. 14, pp. 1951–1954, Nov. 2006, doi: 10.1016/j.ijhydene.2006.01.015.
10. J. A. Okolie, B. R. Patra, A. Mukherjee, S. Nanda, A. K. Dalai, and J. A. Kozinski, "Futuristic applications of hydrogen in energy, biorefining, aerospace, pharmaceuticals and metallurgy," *International Journal of Hydrogen Energy*, vol. 46, no. 13. Elsevier Ltd, pp. 8885–8905, Feb. 19, 2021. doi: 10.1016/j.ijhydene.2021.01.014.
11. S. I. Park, S. M. Jung, J. Y. Kim, and J. Yang, "Effects of Mono- and Bifunctional Surface Ligands of Cu–In–Se Quantum Dots on Photoelectrochemical Hydrogen Production," *Materials*, vol. 15, no. 17, Sep. 2022, doi: 10.3390/ma15176010.
12. A. Fujishima and K. Honda, "Electrochemical Photolysis of Water at a Semiconductor Electrode," *Nature*, vol. 238, no. 5358, pp. 37–38, Jul. 1972, doi: 10.1038/238037a0.
13. M. A. Fox and M. T. Dulay, "Heterogeneous Photocatalysis," 1993. [Online]. Available: https://pubs.acs.org/sharingguidelines
14. A. B. Lavand and Y. S. Malghe, "Visible light photocatalytic degradation of 4-chlorophenol using C/ZnO/CdS nanocomposite," *Journal of Saudi Chemical Society*, vol. 19, no. 5, pp. 471–478, Sep. 2015, doi: 10.1016/j.jscs.2015.07.001.
15. J. Augustyński, B. D. Alexander, and R. Solarska, "Metal oxide photoanodes for water splitting," *Top Curr Chem*, vol. 303, pp. 1–38, 2011, doi: 10.1007/128_2011_135.
16. T. Yui, Y. Tamaki, K. Sekizawa, and O. Ishitani, "Photocatalytic Reduction of CO2: From Molecules to Semiconductors," 2011, pp. 151–184. doi: 10.1007/128_2011_139.
17. S. K. Bajpai, N. Chand, and V. Chaurasia, "Nano Zinc Oxide-Loaded Calcium Alginate Films with Potential Antibacterial Properties," *Food Bioproc Tech*, vol. 5, no. 5, pp. 1871–1881, Jul. 2012, doi: 10.1007/s11947-011-0587-6.
18. A. Fujishima and K. Honda, "Electrochemical evidence for the mechanism of the primary stage of photosynthesis," *Bull Chem Soc Jpn*, vol. 44, no. 4, pp. 1148–1150, 1971.
19. D. S. M. Constantino, M. M. Dias, A. M. T. Silva, J. L. Faria, and C. G. Silva, "Intensification strategies for improving the performance of photocatalytic processes: A review," *Journal of Cleaner Production*, vol. 340. Elsevier Ltd, Mar. 15, 2022. doi: 10.1016/j.jclepro.2022.130800.
20. L. Escobar-Alarcón and D. A. Solís-Casados, "Desarrollo de fotocatalizadores basados en TiO2 en forma de película delgada para la degradación de moléculas orgánicas en solución acuosa," *Mundo Nano. Revista Interdisciplinaria en Nanociencias y Nanotecnología*, vol. 14, no. 26, pp. 1e–23e, Oct. 2020, doi: 10.22201/ceiich.24485691e.2021.26.69646.
21. T. Takata and K. Domen, "Particulate Photocatalysts for Water Splitting: Recent Advances and Future Prospects," *ACS Energy Letters*, vol. 4, no. 2. American Chemical Society, pp. 542–549, Feb. 08, 2019. doi: 10.1021/acsenergylett.8b02209.
22. C. V. Montoya-Bautista, P. Acevedo-Peña, R. Zanella, and R.-M. Ramírez-Zamora, "Characterization and Evaluation of Copper Slag as a Bifunctional Photocatalyst for Alcohols Degradation and Hydrogen Production," *Top Catal*, vol. 64, no. 1–2, pp. 131–141, 2021, doi: 10.1007/s11244-020-01362-4.
23. J. Portier, H. S. Hilal, I. Saadeddin, S. J. Hwang, M. A. Subramanian, and G. Campet, "Thermodynamic correlations and band gap calculations in metal oxides," *Progress in Solid State Chemistry*, vol. 32, no. 3–4, pp. 207–217, 2004.

24. F. Opoku, K. K. Govender, C. G. C. E. van Sittert, and P. P. Govender, "Recent progress in the development of semiconductor-based photocatalyst materials for applications in photocatalytic water splitting and degradation of pollutants," *Adv Sustain Syst*, vol. 1, no. 7, p. 1700006, 2017.
25. M. Mishra and D.-M. Chun, "α-Fe2O3 as a photocatalytic material: A review," *Appl Catal A Gen*, vol. 498, pp. 126–141, 2015.
26. X. Chen, S. Shen, L. Guo, and S. S. Mao, "Semiconductor-based photocatalytic hydrogen generation," *Chem Rev*, vol. 110, no. 11, pp. 6503–6570, Nov. 2010, doi: 10.1021/cr1001645.
27. M. Pelaez *et al.*, "A review on the visible light active titanium dioxide photocatalysts for environmental applications," *Applied Catalysis B: Environmental*, vol. 125. pp. 331–349, Aug. 21, 2012. doi: 10.1016/j.apcatb.2012.05.036.
28. E. Mosquera, N. Carvajal, M. Morel, and C. Marín, "Fabrication of ZnSe nanoparticles: Structural, optical and Raman Studies," *J Lumin*, vol. 192, pp. 814–817, Dec. 2017, doi: 10.1016/j.jlumin.2017.08.017.
29. E. Mosquera, I. Del Pozo, and M. Morel, "Structure and red shift of optical band gap in CdO-ZnO nanocomposite synthesized by the sol gel method," *J Solid State Chem*, vol. 206, pp. 265–271, 2013, doi: 10.1016/j.jssc.2013.08.025.
30. E. Mosquera, C. Rojas-Michea, M. Morel, F. Gracia, V. Fuenzalida, and R. A. Zárate, "Zinc oxide nanoparticles with incorporated silver: Structural, morphological, optical and vibrational properties," *Appl Surf Sci*, vol. 347, pp. 561–568, Aug. 2015, doi: 10.1016/j.apsusc.2015.04.148.
31. X. Guo, L. Liu, Y. Xiao, Y. Qi, C. Duan, and F. Zhang, "Band gap engineering of metal-organic frameworks for solar fuel productions," *Coordination Chemistry Reviews*, vol. 435. Elsevier B.V., May 15, 2021. doi: 10.1016/j.ccr.2021.213785.
32. H. Liang, F. Wang, L. Yang, Z. Cheng, Y. Shuai, and H. Tan, "Progress in full spectrum solar energy utilization by spectral beam splitting hybrid PV/T system," *Renewable and Sustainable Energy Reviews*, vol. 141. Elsevier Ltd, May 01, 2021. doi: 10.1016/j.rser.2021.110785.
33. T. Huanosta-Gutiérrez, R. F. Dantas, R. M. Ramírez-Zamora, and S. Esplugas, "Evaluation of copper slag to catalyze advanced oxidation processes for the removal of phenol in water," *J Hazard Mater*, vol. 213–214, pp. 325–330, Apr. 2012, doi: 10.1016/j.jhazmat.2012.02.004.
34. B. K. Mayer, D. Gerrity, B. E. Rittmann, D. Reisinger, and S. Brandt-Williams, "Innovative strategies to achieve low total phosphorus concentrations in high water flows," *Crit Rev Environ Sci Technol*, vol. 43, no. 4, pp. 409–441, 2013, doi: 10.1080/10643389.2011.604262.
35. R. García-Estrada, S. Arzate, and R.-M. Ramírez-Zamora, "Thiabendazole degradation by photo-NaOCl/Fe and photo-Fenton like processes, using copper slag as an iron catalyst, in spiked synthetic and real secondary wastewater treatment plant effluents," *Water Science and Technology*, vol. 87, no. 3, pp. 620–634, 2023, doi: 10.2166/wst.2022.424.
36. A. A. Morales-Pérez, R. García-Pérez, C. G. Tabla-Vázquez, and R. M. Ramírez-Zamora, "Simultaneous Hydrogen Production and Acetic Acid Degradation by Heterogeneous Photocatalysis using a Metallurgical Waste as Catalyst," *Top Catal*, vol. 64, no. 1–2, pp. 17–25, Jan. 2021, doi: 10.1007/s11244-020-01346-4.
37. L. M. Herrera-Ibarra, R. M. Ramírez-Zamora, A. Martín-Domínguez, M. Piña-Soberanis, D. Schnabel-Peraza, and J. A. Bañuelos-Díaz, "Treatment of Textile Industrial Wastewater by the Heterogeneous Solar Photo-Fenton Process Using Copper Slag," *Top Catal*, vol. 65, no. 9–12, pp. 1163–1179, Aug. 2022, doi: 10.1007/s11244-022-01685-4.
38. C. V. Montoya-Bautista, E. Avella, R. M. Ramírez-Zamora, and R. Schouwenaars, "Metallurgical wastes employed as catalysts and photocatalysts for water treatment: A review," *Sustainability (Switzerland)*, vol. 11, no. 9. MDPI, May 01, 2019. doi: 10.3390/su11092470.
39. M. Solís-López, A. Durán-Moreno, F. Rigas, A. A. Morales, M. Navarrete, and R. M. Ramírez-Zamora, "Assessment of Copper Slag as a Sustainable Fenton-Type Photocatalyst for Water Disinfection," in *Water Reclamation and Sustainability*, Elsevier Inc., 2014, pp. 199–227. doi: 10.1016/B978-0-12-411645-0.00009-2.
40. B. Gorai, R. K. Jana, and Premchand, "Characteristics and utilisation of copper slag - A review," *Resour Conserv Recycl*, vol. 39, no. 4, pp. 299–313, Nov. 2003, doi: 10.1016/S0921-3449(02)00171-4.
41. W. Zhou, X. Liu, X. Lyu, W. Gao, H. Su, and C. Li, "Extraction and separation of copper and iron from copper smelting slag: A review," *J Clean Prod*, p. 133095, 2022.
42. K. S. Barros, V. S. Vielmo, B. G. Moreno, G. Riveros, G. Cifuentes, and A. M. Bernardes, "Chemical composition data of the main stages of copper production from sulfide minerals in Chile: a review to assist circular economy studies," *Minerals*, vol. 12, no. 2, p. 250, 2022.
43. T. C. Phiri, P. Singh, and A. N. Nikoloski, "The potential for copper slag waste as a resource for a circular economy: A review–Part I," *Miner Eng*, vol. 180, p. 107474, 2022.
44. A. P. Nazer, S. Fuentes, O. Pavez, O. Varela, and O. Lanas, "Copper slag tiles. Innovation in clean production.," *Iberoam. J. Proj. Manag.*, vol. 3, no. 2, p. 12, 2012.
45. Q. Zhai, R. Liu, C. Wang, X. Wen, X. Li, and W. Sun, "A novel scheme for the utilization of Cu slag flotation tailings in preparing internal electrolysis materials to degrade printing and dyeing wastewater," *J Hazard Mater*, vol. 424, Feb. 2022, doi: 10.1016/j.jhazmat.2021.127537.

46. C. González, R. Parra, A. Klenovcanova, I. Imris, and M. Sánchez, "Reduction of Chilean copper slags: A case of waste management project," in *Scandinavian Journal of Metallurgy*, Apr. 2005, pp. 143–149. doi: 10.1111/j.1600-0692.2005.00740.x.
47. Z. Guo, D. Zhu, J. Pan, and F. Zhang, "Innovative methodology for comprehensive and harmless utilization of waste copper slag via selective reduction-magnetic separation process," *J Clean Prod*, vol. 187, pp. 910–922, Jun. 2018, doi: 10.1016/j.jclepro.2018.03.264.
48. H. Shen and E. Forssberg, "An overview of recovery of metals from slags," *Waste Management*, vol. 23, no. 10, pp. 933–949, 2003, doi: 10.1016/S0956-053X(02)00164-2.
49. B. S. Kim, S. K. Jo, D. Shin, J. C. Lee, and S. B. Jeong, "A physico-chemical separation process for upgrading iron from waste copper slag," *Int J Miner Process*, vol. 124, pp. 124–127, 2013, doi: 10.1016/j.minpro.2013.05.009.
50. Q. Jin and L. Chen, "A Review of the Influence of Copper Slag on the Properties of Cement-Based Materials," *Materials*, vol. 15, no. 23, p. 8594, Dec. 2022, doi: 10.3390/ma15238594.
51. I. Rohini and R. Padmapriya, "Properties of Bacterial Copper Slag Concrete," *Buildings*, vol. 13, no. 2, p. 290, 2023.
52. W. Wu, W. Zhang, and G. Ma, "Mechanical properties of copper slag reinforced concrete under dynamic compression," *Constr Build Mater*, vol. 24, no. 6, pp. 910–917, Jun. 2010, doi: 10.1016/j.conbuildmat.2009.12.001.
53. C. Lavanya, A. S. Rao, and N. D. Kumar, "Study on Coefficient of Permeability of Copper slag when admixed with Lime and Cement," *IOSR Journal of Mechanical and Civil Engineering*, vol. 7, no. 6, pp. 19–25, 2013.
54. S. Salleh, M. G. Shaaban, H. B. Mahmud, J. Kang, and K. T. Looi, "Production of bricks from shipyard repair and maintenance hazardous waste," *International Journal of Environmental Science and Development*, vol. 5, no. 1, p. 52, 2014.
55. S. Arivalagan, "Experimental study on the flexural behavior of reinforced concrete beams as replacement of copper slag as fine aggregate," *Journal of civil engineering and Urbanism*, vol. 3, no. 4, pp. 176–182, 2013.
56. P. S. Ambily, C. Umarani, K. Ravisankar, P. R. Prem, B. H. Bharatkumar, and N. R. Iyer, "Studies on ultra high performance concrete incorporating copper slag as fine aggregate," *Constr Build Mater*, vol. 77, pp. 233–240, 2015.
57. R. Anudeep, K. V. Ramesh, and V. SowjanyaVani, "Study on mechanical properties of concrete with various slags as replacement to fine aggregate," *Concrete: Aggregate Replacement*, 2015.
58. A. Nazer, J. Payá, M. V. Borrachero, and J. Monzó, "Characterization of Chilean copper slag smelting nineteenth century," *Revista de Metalurgia*, vol. 52, no. 4, p. 083, Dec. 2016, doi: 10.3989/revmetalm.083.
59. W. Wu, W. Zhang, and G. Ma, "Optimum content of copper slag as a fine aggregate in high strength concrete," *Mater Des*, vol. 31, no. 6, pp. 2878–2883, Jun. 2010, doi: 10.1016/j.matdes.2009.12.037.
60. D. Brindha and P. Sureshkumar, "Buckling strength of RCC columns incorporating copper slag as partial replacement of cement," in *Proceedings of National Conference on Emerging Trends in Civil Engineering, Tamil Nadu, India*, 2010.
61. Q. Zhang, B. Zhang, and D. Wang, "Environmental Benefit Assessment of Blended Cement with Modified Granulated Copper Slag," *Materials*, vol. 15, no. 15, p. 5359, Aug. 2022, doi: 10.3390/ma15155359.
62. L. Sun, Y. Feng, D. Wang, C. Qi, and X. Zeng, "Influence of CaO on physical and environmental properties of granulated copper slag: Melting behavior, grindability and leaching behavior," *Int J Environ Res Public Health*, vol. 19, no. 20, p. 13543, 2022.
63. K. Pérez, Á. Villegas, M. Saldaña, R. I. Jeldres, J. González, and N. Toro, "Initial investigation into the leaching of manganese from nodules at room temperature with the use of sulfuric acid and the addition of foundry slag—Part II," *Sep Sci Technol*, vol. 56, no. 2, pp. 389–394, Jan. 2021, doi: 10.1080/01496395.2020.1713816.
64. Y. Shi, Y. Wei, S. Zhou, B. Li, Y. Yang, and H. Wang, "Effect of B2O3 content on the viscosity of copper slag," *J Alloys Compd*, vol. 822, p. 153478, May 2020, doi: 10.1016/j.jallcom.2019.153478.
65. S. Lewowicki and J. Rajczyk, "The usefulness of copper metallurgical slag as a micro-aggegate additive in mortars and concrete mixtures," in *13. International conference on solid waste technology and management. Volume 2.*, 1997.
66. Elizabeth Sangine, "U.S. Geological Survey Mineral commodity summaries Available online: ," https://www.usgs.gov/centers/national-minerals-information-center.
67. M. A. Moram and M. E. Vickers, "X-ray diffraction of III-nitrides," *Reports on Progress in Physics*, vol. 72, no. 3, 2009, doi: 10.1088/0034-4885/72/3/036502.
68. Y. Xue, Z. Guo, D. Zhu, J. Pan, Y. Wang, and R. Zhan, "Efficient utilization of copper slag in an innovative sintering process for Fe-Ni-Cu alloy preparation and valuable elements recovery," *Journal of Materials Research and Technology*, vol. 18, pp. 3115–3129, May 2022, doi: 10.1016/j.jmrt.2022.04.026.
69. T. C. Phiri, P. Singh, and A. N. Nikoloski, "The potential for copper slag waste as a resource for a circular economy: A review–Part II," *Miner Eng*, vol. 172, p. 107150, 2021.

70. Z. Guo, D. Zhu, J. Pan, T. Wu, and F. Zhang, "Improving beneficiation of copper and iron from copper slag by modifying the molten copper slag," *Metals (Basel)*, vol. 6, no. 4, Apr. 2016, doi: 10.3390/met6040086.
71. S. Duan *et al.*, "Efficient photocatalytic hydrogen production from formic acid on inexpensive and stable phosphide/Zn3In2S6 composite photocatalysts under mild conditions," *Int J Hydrogen Energy*, vol. 44, no. 39, pp. 21803–21820, Aug. 2019, doi: 10.1016/j.ijhydene.2019.06.179.
72. C. V. Montoya-Bautista *et al.*, "Photocatalytic H2 Production and Carbon Dioxide Capture Using Metallurgical Slag and Slag-Derived Materials," in *Handbook of Ecomaterials*, Springer International Publishing, 2018, pp. 1–19. doi: 10.1007/978-3-319-48281-1_117-1.
73. P. K. Gbor, V. Mokri, and C. Q. Jia, "Characterization of smelter slags," *J Environ Sci Health A Tox Hazard Subst Environ Eng*, vol. 35, no. 2, pp. 147–167, 2000, doi: 10.1080/10934520009376960.
74. T. S. Gabasiane, G. Danha, T. A. Mamvura, T. Mashifana, and G. Dzinomwa, "Characterization of copper slag for beneficiation of iron and copper," *Heliyon*, vol. 7, no. 4, Apr. 2021, doi: 10.1016/j.heliyon.2021.e06757.
75. T. Chun, C. Ning, H. Long, J. Li, and J. Yang, "Mineralogical Characterization of Copper Slag from Tongling Nonferrous Metals Group China," *JOM*, vol. 68, no. 9, pp. 2332–2340, Sep. 2016, doi: 10.1007/s11837-015-1752-6.
76. M. Sánchez and M. Sudbury, "Physicochemical characterization of copper slag and alternatives of friendly environmental management," *Journal of Mining and Metallurgy, Section B: Metallurgy*, vol. 49, no. 2, pp. 161–168, 2013, doi: 10.2298/JMMB120814011S.
77. H. Tian *et al.*, "Comprehensive review on metallurgical recycling and cleaning of copper slag," *Resources, Conservation and Recycling*, vol. 168. Elsevier B.V., May 01, 2021. doi: 10.1016/j.resconrec.2020.105366.
78. X. Wang, D. Geysen, S. V. P. Tinoco, N. D'Hoker, T. Van Gerven, and B. Blanpain, "Characterisation of copper slag in view of metal recovery," *Transactions of the Institutions of Mining and Metallurgy, Section C: Mineral Processing and Extractive Metallurgy*, vol. 124, no. 2, pp. 83–87, Jun. 2015, doi: 10.1179/1743285515Y.0000000004.
79. A. R. Lori, A. Hassani, and R. Sedghi, "Investigating the mechanical and hydraulic characteristics of pervious concrete containing copper slag as coarse aggregate," *Constr Build Mater*, vol. 197, pp. 130–142, Feb. 2019, doi: 10.1016/j.conbuildmat.2018.11.230.
80. H. Zhang, C. Hu, W. Gao, and M. Lu, "Recovery of iron from copper slag using coal-based direct reduction: Reduction characteristics and kinetics," *Minerals*, vol. 10, no. 11, pp. 1–17, Nov. 2020, doi: 10.3390/min10110973.
81. Y. Diaz-Rosero, L. González-Salcedo, and J. Diaz Rosero, "Caracterización de escoria de cobre secundaria y evaluación de su actividad puzolánica," *Informador Técnico*, vol. 84, no. 2, Mar. 2020, doi: 10.23850/22565035.2696.
82. B. M. Mercado-Borrayo, J. L. González-Chávez, R. M. Ramírez-Zamora, and R. Schouwenaars, "Valorization of Metallurgical Slag for the Treatment of Water Pollution: An Emerging Technology for Resource Conservation and Re-utilization," *Journal of Sustainable Metallurgy*, vol. 4, no. 1. Springer Science and Business Media Deutschland GmbH, pp. 50–67, Mar. 01, 2018. doi: 10.1007/s40831-018-0158-4.
83. C. González, R. Parra, A. Klenovcanova, I. Imris, and M. Sánchez, "Reduction of Chilean copper slags: A case of waste management project," in *Scandinavian Journal of Metallurgy*, Apr. 2005, pp. 143–149. doi: 10.1111/j.1600-0692.2005.00740.x.
84. A. Manasse, M. Mellini, and C. Viti, "The copper slags of the Capattoli Valley, Campiglia Marittima, Italy," *European Journal of Mineralogy*, vol. 13, no. 5, pp. 949–960, Sep. 2001, doi: 10.1127/0935-1221/2001/0013/0949.
85. R. Sáez, F. Nocete, J. M. Nieto, M. Á. Capitán, and S. Rovira, "The extractive metallurgy of copper from Cabezo Juré, Huelva, Spain: Chemical and mineralogical study of slags dated to the third millenium B.C," *Can Mineral*, vol. 41, no. 3, pp. 627–638, 2003, doi: 10.2113/gscanmin.41.3.627.
86. B. Zhang, T. Zhang, and C. Zheng, "Reduction Kinetics of Copper Slag by H2," *Minerals*, vol. 12, no. 5, May 2022, doi: 10.3390/min12050548.
87. T. Kundu, S. Senapati, S. K. Das, S. I. Angadi, and S. S. Rath, "A comprehensive review on the recovery of copper values from copper slag," *Powder Technology*, vol. 426. Elsevier B.V., Aug. 01, 2023. doi: 10.1016/j.powtec.2023.118693.
88. Q. Ma *et al.*, "Performance of copper slag contained mortars after exposure to elevated temperatures," *Constr Build Mater*, vol. 172, pp. 378–386, May 2018, doi: 10.1016/j.conbuildmat.2018.03.261.
89. A. Lasia, "Semiconductors and Mott-Schottky Plots," in *Electrochemical Impedance Spectroscopy and its Applications*, Springer New York, 2014, pp. 251–255. doi: 10.1007/978-1-4614-8933-7_10.
90. R. Gómez and T. Lana-Villarreal, "Tema 3. Conceptos de cinética electroquímica," *Corrosión*, 2008.
91. B. Tian, Q. Lei, B. Tian, W. Zhang, Y. Cui, and Y. Tian, "UV-driven overall water splitting using unsupported gold nanoparticles as photocatalysts," *Chemical Communications*, vol. 54, no. 15, pp. 1845–1848, 2018.
92. S. Nandy, S. A. Savant, and S. Haussener, "Prospects and challenges in designing photocatalytic particle suspension reactors for solar fuel processing," *Chemical Science*, vol. 12, no. 29. Royal Society of Chemistry, pp. 9866–9884, Aug. 07, 2021. doi: 10.1039/d1sc01504d.

93. C. D. Fernández-Solis *et al.*, "Fundamentals of electrochemistry, corrosion and corrosion protection," *Soft Matter at Aqueous Interfaces*, pp. 29–70, 2016.
94. E. McCafferty, "Validation of corrosion rates measured by the Tafel extrapolation method," *Corros Sci*, vol. 47, no. 12, pp. 3202–3215, 2005.
95. J. W. Halley, A. Schofield, and B. Berntson, "Use of magnetite as anode for electrolysis of water," *J Appl Phys*, vol. 111, no. 12, 2012.
96. Y. J. Zhang and Q. Chai, "Alkali-activated blast furnace slag-based nanomaterial as a novel catalyst for synthesis of hydrogen fuel," *Fuel*, vol. 115, pp. 84–87, 2014, doi: 10.1016/j.fuel.2013.06.051.
97. B. Tian, Q. Lei, W. Zhang, Y. Cui, Y. Tian, and B. Tian, "UV-driven overall water splitting using unsupported gold nanoparticles as photocatalysts," *Chemical Communications*, vol. 54, no. 15, pp. 1845–1848, 2018, doi: 10.1039/c7cc09770k.
98. C. Xu, P. Ravi Anusuyadevi, C. Aymonier, R. Luque, and S. Marre, "Nanostructured materials for photocatalysis," *Chemical Society Reviews*, vol. 48, no. 14. Royal Society of Chemistry, pp. 3868–3902, Jul. 21, 2019. doi: 10.1039/c9cs00102f.
99. C. V. Montoya-Bautista *et al.*, "Photocatalytic H2 Production and Carbon Dioxide Capture Using Metallurgical Slag and Slag-Derived Materials," in *Handbook of Ecomaterials*, Springer International Publishing, 2018, pp. 1–19. doi: 10.1007/978-3-319-48281-1_117-1.
100. S. Y. Arzate-Salgado, A. A. Morales-Pérez, M. Solís-López, and R. M. Ramírez-Zamora, "Evaluation of metallurgical slag as a Fenton-type photocatalyst for the degradation of an emerging pollutant: Diclofenac," in *Catalysis Today*, Elsevier B.V., May 2016, pp. 126–135. doi: 10.1016/j.cattod.2015.09.026.
101. J. H. Kim, D. Hansora, P. Sharma, J. W. Jang, and J. S. Lee, "Toward practical solar hydrogen production-an artificial photosynthetic leaf-to-farm challenge," *Chemical Society Reviews*, vol. 48, no. 7. Royal Society of Chemistry, pp. 1908–1971, Apr. 07, 2019. doi: 10.1039/c8cs00699g.
102. C. C. Lo, C. W. Huang, C. H. Liao, and J. C. S. Wu, "Novel twin reactor for separate evolution of hydrogen and oxygen in photocatalytic water splitting," *Int J Hydrogen Energy*, vol. 35, no. 4, pp. 1523–1529, Feb. 2010, doi: 10.1016/j.ijhydene.2009.12.032.
103. I. Dincer, "Green methods for hydrogen production," in *International Journal of Hydrogen Energy*, Jan. 2012, pp. 1954–1971. doi: 10.1016/j.ijhydene.2011.03.173.
104. M. E. Borges, S. Navarro, H. de Paz Carmona, and P. Esparza, "Natural Volcanic Material as a Sustainable Photocatalytic Material for Pollutant Degradation under Solar Irradiation," *Materials*, vol. 15, no. 11, Jun. 2022, doi: 10.3390/ma15113996.
105. L. Li, R. Chen, Q. Liao, X. Zhu, G. Wang, and D. Wang, "High surface area optofluidic microreactor for redox mediated photocatalytic water splitting," in *International Journal of Hydrogen Energy*, Elsevier Ltd, Nov. 2014, pp. 19270–19276. doi: 10.1016/j.ijhydene.2014.05.098.
106. H. Nishiyama *et al.*, "Photocatalytic solar hydrogen production from water on a 100-m2 scale," *Nature*, vol. 598, no. 7880, pp. 304–307, Oct. 2021, doi: 10.1038/s41586-021-03907-3.